Rational design of O/W nanoemulsions based on the surfactant dodecyldiglyceryl ether using the normalized HLD concept and the formulation-composition map

Lucie Delforce, Jesus Ontiveros, Véronique Rataj, Jean-Marie Aubry

Rational design of O/W nanoemulsions based on the surfactant dodecyldiglyceryl ether using the Normalized HLD concept and the Formulation-Composition map

Lucie Delforce, Jesús F. Ontiveros, Véronique Nardello-Rataj*, Jean-Marie Aubry*

Univ. Lille, CNRS, Centrale Lille, Univ. Artois, UMR 8181 - UCCS – Unité de Catalyse et Chimie du Solide, F-59000 Lille, France

Abstract

The 1-O-dodecyl diglycerol ether ($C_{12}Gly_2$) is a well-balanced bio-based surfactant whose amphiphilicity and emulsifying property have been studied within the Normalized Hydrophilic-Lipophilic-Deviation (HLD_N) framework. Its Hydrophilic-Lipophilic tendency has been measured in saline and salt-free media by two methods. The classic one, is based on the identification of the optimal formulation (Winsor III) in a series of tubes containing a series of $C_{12}Gly_2$/Alkane/Water systems at equilibrium. The alternative method, much faster and more precise, is based on the phase inversion of the same systems under stirring, the HLD_N value of which is gradually modified by changing the temperature or the salinity. $C_{12}Gly_2$ is found to be three times less sensitive to temperature and salinity variations than typical ethoxylated surfactants.

By stirring $C_{12}Gly_2$/Alkane/Water systems, O/W or W/O emulsions are obtained depending on whether the alkane is long or short. The finest and the least stable emulsions (1 µm) are obtained with n-octane for which $HLD_N = 0$. By systematically varying the water-to-oil ratio (WOR) and the hydrophobicity of the oil, either direct O/W or reverse W/O emulsions are formed and are represented in a Formulation-Composition map. This map is a powerful tool to guide the formulator about which type of emulsion will be obtained depending on the composition of the SOW system and the emulsification protocol used i.e. the pathway in the map. In particular, it is possible to prepare stable and very fine emulsions (≈ 100 nm) by crossing the inversion border of the map favouring the splitting of the droplets and then moving away from it quickly to prevent the coalescence of the droplets.

Keywords*: Bio-based surfactant, HLD_N, Formulation-Composition Map, Nanoemulsion*

1. Introduction

The bio-based 1-*O*-dodecyl diglyceryl ether ($C_{12}Gly_2$) surfactant, shown in Figure 1, was previously reported as an effective solubilizing agent providing Winsor III microemulsions at low concentration and as a promising emulsifying agent forming smaller droplets than the polyethoxylated fatty alcohol $C_{12}E_6$.[1,2] Its emulsifying properties are further investigated in this work, in particular the rationalization of emulsion properties in relation with the normalized Hydrophilic Lipophilic Deviation (HLD) equation, noted HLD_N.

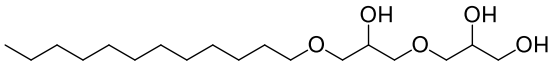

Figure 1. 1-*O*-dodecyl diglyceryl ether surfactant structure.

For designing emulsions of desired morphology and stability, several methodologies are available. In the past century, Ostwald showed that the Water-to-Oil Ratio (WOR) drives emulsion morphology when WOR is significantly different from 1, the emulsion continuous phase tends to be the phase present in larger amount.[3] On the contrary, Bancroft showed that when WOR is not too far from 1, the morphology of the emulsion is mainly driven by the affinity of the surfactant for the oil or aqueous phase. As a result, when agitating SOW systems with a hydrophilic (or lipophilic) surfactant, the resulting emulsion morphology is O/W (or W/O).[4,5] Since then, many theoretical and practical tools have been developed to quantify the hydrophilic-lipophilic tendency of surfactants in SOW systems, the most widely used still being the empirical Hydrophilic-Lipophilic Balance (HLB) of Griffin. For his part, Salager developed the Hydrophilic-Lipophilic Deviation equation, abbreviated as HLD, which describes much better the phase behaviour of emulsions and microemulsions as a function of the nature of the surfactant and the oil as well as the influence of the temperature and salinity. Recently, a simplified and more meaningful version of the HLD has been designed and called the Normalized Hydrophilic-lipophilic deviation (HLD_N)[6–8]. The variation of the HLD_N as a function of the variables capable of modifying the affinity of the surfactant for oils or for water is given by equation (1) for nonionic surfactants.

$$HLD_N = PACN - EACN + \tau(T - 25) + \delta S \quad (1)$$

where PACN (Preferred Alkane Carbon Number) expresses the hydrophilic-lipophilic tendency of the surfactant. It is equal to the length of the n-alkane forming a Winsor III microemulsion at 25°C in salt-free solution. EACN characterizes the hydrophobicity of the oil and is equal to the number of carbon atoms (ACN) when the oil is an n-alkane. T is the temperature (°C) and S the salinity (wt.% NaCl). τ and δ coefficients reflect the surfactant sensitivity towards temperature and salinity, respectively.

Both temperature and salinity sensitivity are properties of interest for the formulation of end-use products. Indeed, stability must be ensured over a range of temperature for storage.

Moreover, the sensitivity of surfactants towards salts is a key parameter for formulating some personal care products or detergents as adjusting salinity modifies the surfactant packing parameter, changing from spherical to worm-like micelles in detergents and shampoos, increasing viscosity to facilitate the use of the product. The HLD_N equation considers the contribution of formulation variables to the relative affinity of surfactant for either the aqueous or the oil phase. When $HLD_N < 0$, the affinity of the surfactant is stronger towards the aqueous phase, when $HLD_N > 0$, the affinity is stronger towards the oil phase and when $HLD_N = 0$, the system is called to be at the "optimum formulation".[9] In this case, the average curvature of the interfacial film is zero because the surfactant has an equal affinity for the aqueous and the oil phases. A three-phase system (Winsor III) then forms spontaneously when such SOW mixture equilibrates[10], because the interfacial tension O/W is ultra-low [11–14]. At the same time, when these optimal systems are stirred, the stability of the emulsions then formed is minimal as well as their viscosity.[15]

When temperature is the formulation variable, $HLD_N = 0$ is reached at an equilibrium temperature T*, which is similar to the phase inversion temperature (PIT) introduced by Shinoda et al.,[16] when the surfactants are pure. The same way, when salinity is the formulation variable, $HDL_N = 0$ is reached at the salinity S*, similar to the salinity of phase inversion (SPI) in a dynamic system when the water/oil ration is close to 1. The parameters expressing the sensitivity towards temperature (τ) and salinity (δ) are usually determined from the SOW-T and SOW-S fish diagrams studied with a series of *n*-alkanes as oils, but reaching the thermodynamic equilibrium is a long process and such experimental determination is time-consuming. Instead, dynamic inversion approaches were chosen in this work to determine PACN, τ and δ for $C_{12}Gly_2$.

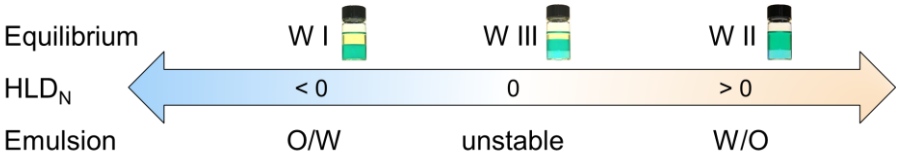

Figure 2. Illustration of SOW systems behaviour with HLD_N evolution when emulsified (bottom) and at equilibrium (top).

According to equation (1), the nature of the oil can be tuned to obtain either O/W ($HLD_N < 0$) or W/O ($HLD_N > 0$) emulsions for which stability evolution can be anticipated, as shown in Figure 2. Other factors such as the emulsification process, the WOR and the surfactant concentration were also studied for comparison purposes. In this way, the scope of application of the glycerol-based 1-*O*-dodecyl diglyceryl ether ($C_{12}Gly_2$) surfactant was investigated: the resulting emulsions were characterized in terms of morphology, granulometry and stability.

2. Materials and methods

2.1. Chemicals

Cyclohexane (> 99.5%), cyclooctane (> 99%), octane (98%), nonane (99%), and hexadecane (99%) were purchased from Sigma-Aldrich. Hexane (> 99%) was supplied by Acros organics, heptane (99%), decane (99%) and dodecane (99%) were supplied from Alfa Aesar, undecane (> 99%), tetradecane (> 99%) and squalane (> 98%) were obtained from TCI. Octyl octanoate (>98%) was purchased from SAFC®. Pure tetraethyleneglycol monodecyl ether ($C_{10}E_4$) used as the reference surfactant was synthesized according to a method described elsewhere.[17,18] Its purity was assessed by GC-MS analysis (> 99%) and by comparing its cloud point temperature (20.4 C at 2.6 wt.%) with the reference value (20.6 C at 2.6wt%).[19]

1-O-dodecyl diglyceryl ether ($C_{12}Gly_2$, 98%) was synthesized according to the procedure previously described.[20]

2.2. Phase Inversion Temperature (PIT)

$C_{12}Gly_2$ (0.085 g), *n*-alkane (4.25 g) and aqueous NaCl 10^{-2} M (4.25 g) were introduced in a double-jacketed cylindrical tube (d = 2.5 cm, h = 20 cm). The system 1 wt.% $C_{12}Gly_2$/*n*-alkane/water was briefly stirred and left to pre-equilibrate at room temperature. The system was cooled down to 18 C for 10 minutes and kept under stirring at 500 rpm using a 2 cm-square-cross magnetic stirrer during the whole experiment. Two heating and cooling cycles were then applied at a rate of 1°C/min up to 60°C by circulating water in the vessel using a HUBER 125 Ministat. Conductivity was recorded using a CDM210 conductivity meter from MeterLab® with a coupled conductivity-temperature electrode CDC641T from Radiometer Analytical®. Conductivity data were processed with the Labview software.

2.3. Salinity of Phase Inversion (SPI)

The general procedure and experimental vessel used for dynamic salinity phase inversion was described by Lemahieu et al.[21,22] $C_{12}Gly_2$ (0.085 g), *n*-alkane (4.25 g) and water (4.25 g) were introduced in a double-jacketed cylindrical tube (d = 2.5 cm, h = 20 cm). This 1 wt.% $C_{12}Gly_2$/*n*-alkane/water mixture was briefly stirred and left to pre-equilibrate 1 h at 20.0°C. Dynamic phase inversions are induced by increasing or decreasing continuously the aqueous phase salinity. An aqueous solution of NaCl at 25 wt.% (d = 1.19) or pure water (d = 1) and $C_{12}Gly_2$ (2%) in *n*-alkane are added using two single syringe infusion pumps (Legato® 100 Syringe Pump, KD Scientific) at constant rate of 0.059 g/min so as to maintain the WOR weight equal to 1 and the surfactant concentration equal to 1%. The mixture is stirred using a 2 cm-cross magnetic stirrer and temperature is maintained at 20.0°C by circulating water controlled by a HUBER® 125 Ministat. Phase inversions are monitored by electrical conductivity measurement as described in the previous paragraph.

2.4. Emulsions and characterization protocol

2.4.1. Preparation

The surfactant was dissolved in oil and the mixture surfactant/oil was sonicated and heated if necessary. Then the NaCl 10^{-2} M solution (aqueous phase) was slowly added. In the first series of experiments, the mixture was agitated using an Ultra-turrax® (IKA T18/S18N-10G) at 3000 rpm for 5 minutes. For studying the influence of emulsification process, a second series of experiments was carried out using a phase inversion procedure. In that case, the mixture was kept under stirring at 500 rpm using a 2 cm-square-cross magnetic stirrer. For emulsions containing hexane, heptane or octane, the temperature was set to PIT+5°C, cooled down to PIT-5°C at a rate of 1°C/min and heated up to 25°C at 2°C/min. For emulsions containing nonane, decane, dodecane or tetradecane, the temperature was set to PIT-5°C, increased to PIT+5°C at a rate of 1°C/min and cooled down to 25°C at 2°C/min. In all cases, emulsion morphology was assessed by conductivity measurements. 1 mL sample was taken for size measurements and the emulsion was placed in a Turbiscan® AGS from Formulaction for 14 to 28 days.

For the phase inversion temperature and dilution experiments of dodecane/water emulsions, mixtures containing water and dodecane (water volume fraction of 0.2) and either 2.9% $C_{12}Gly_2$ or 8.5% $C_{12}Gly_2$ were prepared, heated from room temperature up to 55°C at a rate of 2°C/min, and cooled down by quick addition of a NaCl 10^{-2} M solution at 10°C to reach a water fraction of 0.7. The final mixtures contain 1% and 3% of $C_{12}Gly_2$, respectively.

2.4.2. Droplet size

Droplet size distribution was measured using a Mastersizer® 3000 laser granulometer from Malvern Panalytical when an O/W emulsion was formed. When a W/O emulsion was obtained, the emulsion was observed at the optical microscope (Keyens VHX-900F). In that case, size distribution was calculated from at least 500 droplets per emulsion, grouped in 100 size intervals. $D_{[4,3]}$ is given as $\sum N_i D_i^4 / \sum N_i D_i^3$ where N_i is the number of observations in the size interval i of mean diameter D_i. For smaller emulsions with droplets about 1 µm, size was also measured by Dynamic Light Scattering using a Zetasizer Nano® ZS from Malvern Panalytical. In that case, $D_{[4,3]}$ corresponded to the mean D_v diameter value. After stability monitoring, emulsions were gently re-homogenized by hand and size distributions were re-measured according to the procedures described above.

2.4.3. Stability

Samples were scanned top to bottom by a laser beam (λ = 880 nm) using a Turbiscan® AGS equipped with an auto-sampling robot capable of analysing up to 54 samples maintained at constant temperature. Detectors placed at angles of 180° and 45° record the transmitted (*T*) and back-scattered (*BS*) light along the sample height. 54 samples can be stored at

controlled temperature and monitored at the same time. At regular time intervals (every 12 h), samples were taken by the automatic robotic arm and placed in the analysis chamber, and placed back in the 25.0°C storage station until the next analysis. Stability data was then processed using the Turbisoft treatment software, from which many destabilization indicators could be computed. *T* and *BS* light signals allowed visualizing the evolution of opaque and clear area over time. Indeed, the intensity of *T* and *BS* directly depend on the concentration and size of light scattering objects according to equations (2) and (3).[23]

$$T = T_0 \exp\left(\frac{-3r_i\phi Q_e(d)}{d}\right) \quad (2)$$

$$BS = \alpha\sqrt{\frac{3\phi(1-g(d))Q_e(d)}{2d}} + \beta \quad (3)$$

with T_0 the transmitted signal of the continuous phase, r_i the internal radius of the measurement cell, d the particle mean size, ϕ the volume fraction of dispersed phase, Q_e the extinction efficiency, α and β the gain and offset of the experimental setup and g the asymmetry factor that quantifies the anisotropy of the light scattered by dispersed objects.

In this work, the evolution of internal phase released over time was calculated as an indicator of emulsion destabilization. In practice, it was obtained by measuring the peak width of T signal at a threshold of $T = T_{max}/10$ at the top (O/W) or at the bottom (W/O) of the sample over time. The relative released volume (%) was calculated as the ratio between the volume of release internal phase and the initial volume introduced in the emulsion.

3. Results and discussion

The bio-based surfactant 1-O-alkyl diglyceryl ethers can be obtained by a sustainable synthetic route described by Shi et al. [24]. It involves a catalytic reductive etherification of diglycerol with linear aldehydes to produce a mixture of 1-O-alkyl diglyceryl ethers and 2-O-alkyl diglyceryl ethers (selectivity > 9/1). However, the presence of 2-O-dodecyl diglyceryl ether causes slight changes in physicochemical properties (see Supplementary Information). We therefore preferred to use for our study a sample of pure 1-O-alkyl diglyceryl ethers prepared by a more selective alternative synthesis route described by Delforce et al.[20]

3.1. Temperature and salinity sensitivity (HLD_N parameters)

In this section, the HLD_N parameters of $C_{12}Gly_2$ are determined by resorting to the phase inversion induced either by temperature (PIT) or salinity (SPI) scan in water/n-alkane systems. τ and δ correspond to the HLD_N variation triggered by a change of 1°C or 1 wt.% NaCl and are determined by studying the T and S conditions for which the phase inversion is reached ($HLD_N = 0$).

Dynamic PIT conductivity profiles are shown in the top of Figure 3a for WOR 50-50 emulsions obtained with linear alkanes ranging from octane to dodecane. As expected, the PIT value increases with ACN, as the oil hydrophobicity increases: intermolecular interactions between alkane molecules are stronger and the penetration of the surfactant is decreased. At the bottom of Figure 3a, we can compare the PIT values of $C_{12}Gly_2$ with $C_{10}E_4$ surfactant at different ACN. According to equation (1), the temperature coefficient can be obtained as the slope of the ACN *vs.* PIT. The PIT value increases with ACN, resulting in smaller τ value (see Figure 3a).

The PIT evolution as a function of the n-alkane length also provides the surfactant PACN value which is the ACN number corresponding to a PIT value of 25 C without alcohol nor salt. The PACN corresponds to the carbon number of the *n*-alkane leading to a minimum interfacial tension, i.e. the optimum formulation.[25] It should be noticed that both $C_{10}E_4$ and $C_{12}Gly_2$ have similar values of PACN (8.1-8.3 for $C_{10}E_4$ [22,26,27] and 8.2 for $C_{12}Gly_2$) as they form spontaneously a Winsor III system with n-octane at 25°C. That is why $C_{10}E_4$ was selected for comparison with $C_{12}Gly_2$. However, their behaviour differs greatly when temperature varies. $C_{12}Gly_2$ being three times less “sensitive”, with a τ value of 0.14 C^{-1} against 0.40°C^{-1} for $C_{10}E_4$, inversions require more thermic energy to occur. All C_iE_j surfactants with an alkyl chain length of at least 10 carbons have τ and δ parameters of the same orders of magnitude [8,22] but those results show that not all nonionic polar heads have the same impact on temperature sensitivity. Ontiveros et al. [28] reported a $C_{12}Gly_2$ PACN value of 8 determined by phase equilibrium, 7.2 by the PIT-slope method, assuming that the temperature coefficient was identical to that of $C_{10}E_4$, and 7.3 by the PIT-slope method assuming temperature coefficients were different but the surfactant mixture followed a linear mixing rule. Those three values agree well with ours as the $C_{12}Gly_2$ concentration is low in the PIT-slope method, limiting the error to an acceptable margin.

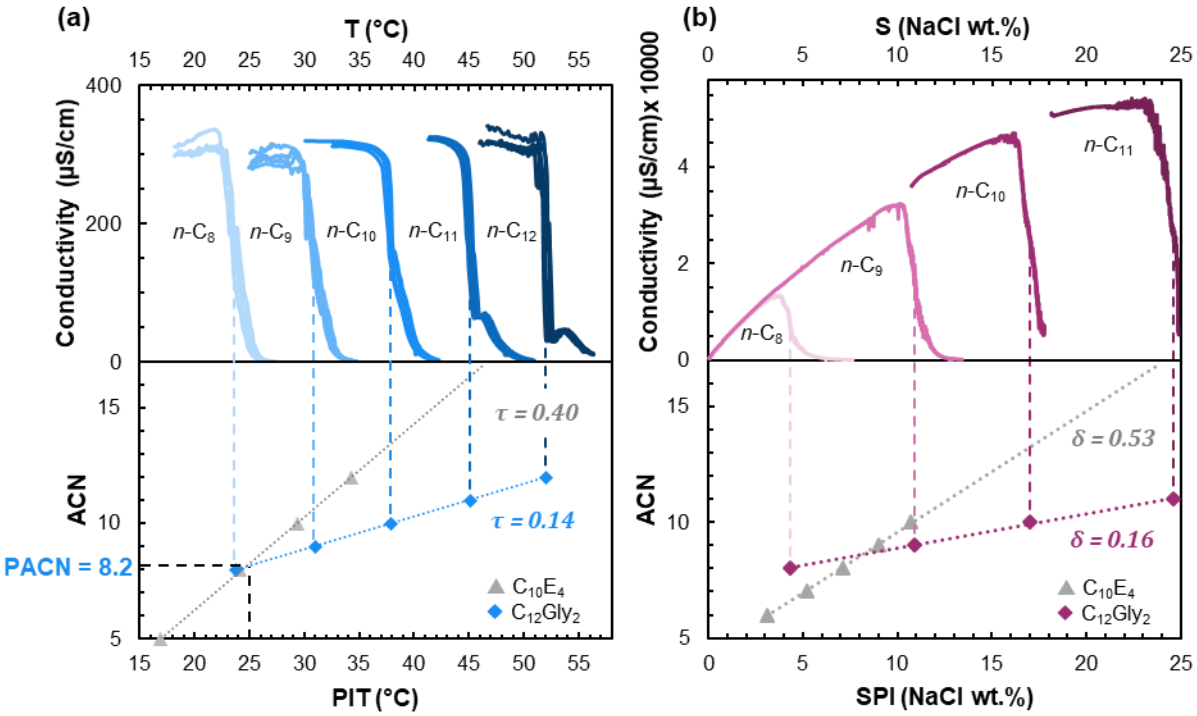

Figure 3. Conductivity monitored dynamic phase inversion triggered by (a) temperature (PIT) at a salinity of 10^{-2} M NaCl and (b) salinity (SPI) at a temperature of 20.0°C variations and their evolution depending on the n-alkane length (ACN). Emulsions are prepared at WOR=1 and the oil nature is varied from octane (ACN = 8) to dodecane (ACN = 12) or undecane in salinity screening due to NaCl solubility limitations. The τ coefficient obtained by PIT[22] and δ coefficient obtained by SPI[22] are represented for $C_{10}E_4$ for comparison.

Temperature sensitivity of nonionic surfactants is due to the formation/cleavage of hydrogen bonds between the polar head and water. As T increases, so does molecular agitation, breaking hydrogen bonds and thus reducing the affinity of surfactant-for water. In C_iE_j surfactants, ether -O- groups are mostly responsible for the hydrophilicity of the polar head since it contains four ether groups and only one terminal hydroxyl -OH. In contrast, $C_{12}Gly_2$ contains two ether bonds and three hydroxyl groups. As the hydrogen bonds between the hydroxyl groups (-OH) and water are significantly stronger than the H-bonds between the ether functions (-O-) and water, the cleavage of the hydrogen bonds of $C_{12}Gly_2$ requires more thermal energy (higher temperature) than $C_{10}E_4$.[29]

Dynamic conductivity profiles for salinity phase inversion with different *n*-alkanes are presented in the top of Figure 3b. In the bottom of Figure 3b, the SPI evolution with ACN for $C_{12}Gly_2$ is compared to that for $C_{10}E_4$. Using equation (1), the salinity coefficient "δ" can be calculated. The salinity sensitivity is significantly higher for the polyethoxylated surfactant (δ $C_{12}Gly_2$ = 0.16 wt.%$^{-1}$ against 0.53 wt.%$^{-1}$). By NaCl salt addition, the activity of water is reduced: hydration of Na^+ and Cl^- ions requires several water molecules per ion, at the expense of the hydration of the polar heads of surfactants.[30] As more H-bond interactions are formed between $C_{12}Gly_2$ and water than between $C_{10}E_4$ and water, the salinity sensitivity of $C_{10}E_4$ is about three times as high as that of $C_{12}Gly_2$.

3.2. Emulsifying properties of $C_{12}Gly_2$

Very few publications describe the use of alkylglyceryl ethers as emulsifiers. In 1989, Sagitani et al.[1] compared the efficiency of 3 wt.% $C_{12}Gly_2$ and $C_{12}EO_6$ as emulsifiers in dodecane / H_2O (2:8 wt.) systems. They showed that the droplet size was much smaller (0.47 µm against 1.28 µm) in the case of $C_{12}Gly_2$, even though the emulsification protocol is unclear. Further understanding of this behaviour was investigated in this work. The HLD_N value of a SOW systems gives precious information regarding the surfactant affinity towards the aqueous or the oil phase, and the resulting Winsor phase behaviour at equilibrium. Salager et al.[7] established that the morphology and stability of emulsions depend on the HLD_N value (formulation variables), the surfactant concentration and the WOR of the system (concentration variables) and finally in the agitation protocol (process variables).

3.2.1. Granulometry and stability of emulsions rationalized by HLD_N evolution

The influence of the oil, characterized by the EACN value, was investigated in the framework of the HLD_N theory. The water-to-oil ratio (WOR) was varied and emulsions were agitated using an Ultra-turrax® according to the procedure described in the experimental section. Stability monitoring of the emulsions was achieved using a Turbiscan so as to detect the different processes involved in emulsion destabilization.

Droplet granulometry is an indicator of the dispersibility of one phase in the other: the lower the interfacial tension, the smaller the resulting droplets.[31] $D_{[4,3]}$ measured in emulsions formed with oils of varying EACN from 2 to 16, are presented in Table 1 and Figure 4. As expected, droplets are smaller close to $HLD_N = 0$, i.e. EACN = 8, corresponding to an interfacial film with zero curvature, favouring an efficient deformation of phases. $HLD_N = 0$ also corresponds to a minimum in interfacial tension, improving the mixing efficiency.[11–15,32] The slow evolution of $C_{12}Gly_2$ emulsions after preparation allowed measuring droplet size including with octane although the destabilization is supposedly much faster when HLD_N is close to 0.[33] Size distributions, available in the Supplementary Information, are similar for most samples and wider for hexane and decane emulsions, close to $HLD_N = 0$, as droplets of about 1 µm are formed in addition to larger ones.

Table 1. Droplet $D_{[4,3]}$ of emulsions containing 1 wt.% $C_{12}Gly_2$ and prepared by varying the nature of the oil and the Water-to-Oil Ratio (wt./wt.). Corresponding volume water fraction is indicated in brackets. $D_{[4,3]}$ are measured 5 minutes after preparation.

Oil	EACN	HLD_N	$D_{[4,3]}$ (µm) and (volume water fraction) at WOR				
			20-80	30-70	50-50	70-30	80-20
cyclohexane	2.1	6.1	48.8 (0.16)	55.9 (0.25)	34.8 (0.44)	15.2 (0.65)	7.5 (0.76)

cyclooctane	4.1	4.1	36.9 (0.17)	31.4 (0.26)	21.5 (0.45)	11.4 (0.66)	5.2 (0.77)
hexane	6	2.2	18.2 (0.14)	17.9 (0.22)	16.8 (0.40)	9.8 (0.60)	3.5 (0.72)
octane	8	0.2	2.9 (0.15)	1.9 (0.23)	1.7 (0.41)	1.5 (0.62)	2.0 (0.74)
decane	10	-1.8	6.5 (0.15)	7.6 (0.24)	21.4 (0.42)	11.8 (0.63)	14.2 (0.74)
dodecane	12	-3.8	8.6 (0.16)	13.7 (0.24)	28.8 (0.43)	19.3 (0.64)	24.4 (0.75)
tetradecane	14	-5.8	11.5 (0.16)	17.6 (0.25)	27.1 (0.43)	30 (0.64)	33.8 (0.75)
hexadecane	16	-7.8	12.3 (0.16)	20.7 (0.25)	32.8 (0.44)	34.4 (0.64)	36.0 (0.76)

Based on $D_{[4,3]}$ measurements, iso-granulometry curves shown in Figure 4 were calculated and presented in a Formulation - Composition map. Interfacial tension being minimal when EACN = PACN, phases are efficiently mixed and small droplets are formed. This is confirmed for all the WOR investigated, the smallest droplets are obtained with octane (ACN = 8) which is the *n*-alkane closest to the PACN of $C_{12}Gly_2$ (8.2). In the same way, droplet size increases as EACN differs from PACN. For several systems described in the literature and containing medium chain alcohols in the formulation, there are 2 minimums on the droplet size, one on each side of the optimal formulation.[34,35] The alcohol role in the formulation is to avoid the liquid crystal formation and/or modify the hydrophilicity of the system. In our case, the absence of alcohol and the presence of liquid crystals in the aqueous phase explains that there is only a minimum as in the ethoxylate nonylphenol/kerosene/water emulsions described by Tolosa et al.[35]

Interestingly, no catastrophic phase inversion was observed for emulsions with extreme WOR ranging up to 80-20 and down to 20-80, and catastrophic inversion occurs beyond these boundaries. For WOR 20-80 and 80-20, the High Internal Phase Emulsions (HIPE) have smaller droplets than the other emulsions obtained with the same oil and the same emulsification procedure but with WOR values closer to 1. The catastrophic phase inversion boundary was determined by stirring systems increasingly rich in internal phase until no stable emulsion was formed. In Figure 4, these inversion boundaries are shown as two thick and gray vertical lines. Beyond these boundaries, no stable emulsion is obtained because there is a conflict between the physicochemistry which favours one type of emulsion (Bancroft's rule) and the extreme values of the WOR which favour the other type of emulsions (Otswald’s rule).

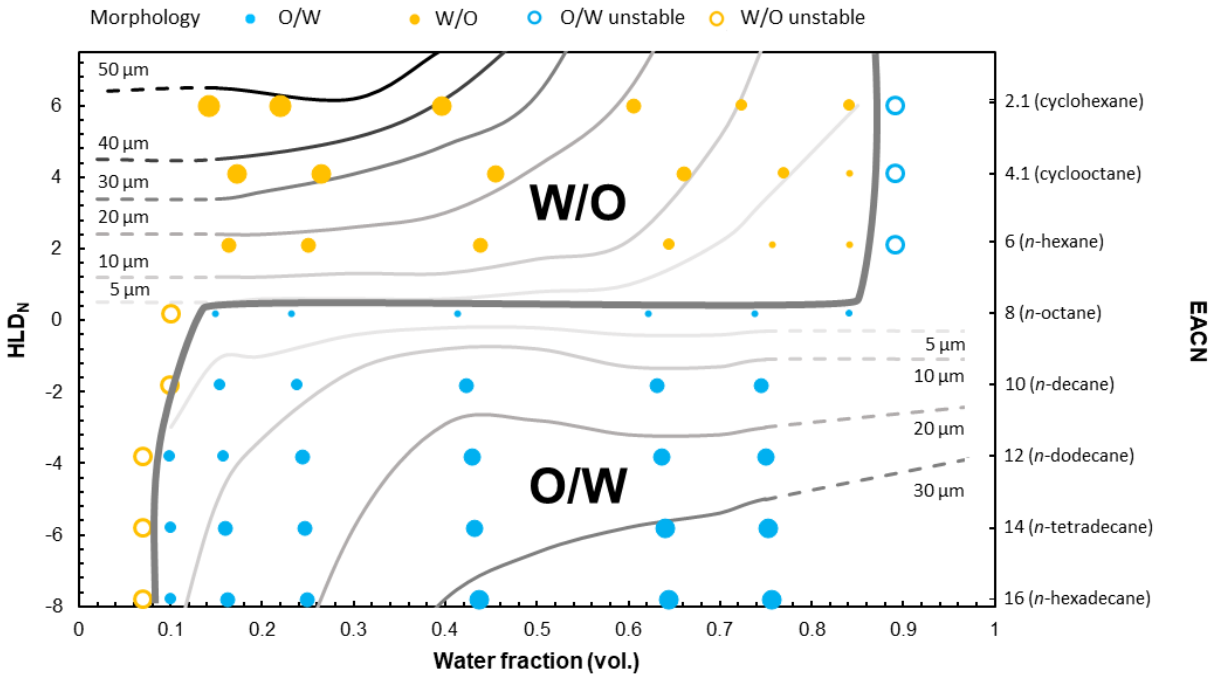

Figure 4. Iso-granulometry curves of emulsions containing 1 wt.% $C_{12}Gly_2$ and prepared by varying the nature of the oil (EACN) and the water fraction (vol.) at 25°C. Droplet $D_{[4,3]}$ are measured 5 minutes after emulsification. O/W and W/O emulsions are represented by blue dots and yellow dots respectively and symbol size is varied with $D_{[4,3]}$ values. The standard inversion line separating O/W and W/O areas is represented as the continuous thick grey line.

$C_{12}Gly_2$ is a well-balanced non-ionic surfactant providing either O/W or W/O emulsions at room temperature by only varying the nature of the oil. These results made it possible to construct a Formulation-Composition map, original in that the scanning variable used to change the HLD_N value is the hydrophobicity (i. e. the EACN) of the oil. As far as we know, this is the first map of this type since the usual scanning variables are the temperature, the salinity of the aqueous phase or the number of ethoxylates of the non-ionic surfactants.

For WOR 50/50, the O/W and W/O drop sizes for water/hexane and decane/water emulsions are 17 and 21 µm, respectively. Water drops will move faster in hexane (viscosity of 0.28 mPa.s) than decane drops in water (1 mPa.s). Moreover, the density difference between the liquids is also higher between the water/hexane mixture (0.655 vs. 1 g/mL) than between the water/decane system (0.73 vs 1 g/mL). The sedimentation of water drops in hexane is favoured over the creaming of decane drops in water. Comparing W/O (cyclohexane and cyclooctane) with the O/W emulsions, there is a slight internal phase release for W/O emulsions at low WOR (20-80) corresponding to the largest droplet sizes shown in Figure 4. On the contrary, O/W emulsions (dodecane, tetradecane and hexadecane) at high WOR (80-20) did not, even though droplet sizes were comparable with those of W/O emulsions for EACN very different from PACN. O/W droplet interfaces seems to be thus better stabilized than W/O ones, probably due to high solubility of $C_{12}Gly_2$ in

cyclohexane and cyclooctane compared to its solubility in water. Indeed, solubilization of the surfactant in the bulk continuous phase reduces the effective concentration of surfactant adsorbed at the droplets interface, destabilizing the droplets. This is supported by the absence of significant internal phase release for WOR higher than 20-80 in W/O emulsions: when the amount of oil is decreased, the fraction of $C_{12}Gly_2$ solubilized in the continuous phase is also reduced and droplet interface stability is improved.

Stability monitoring with static multiple light scattering (Turbiscan®) allows identifying the phenomena involved in emulsion destabilization, as shown in Figure 5. First of all, due to density differences, emulsions tend to cream (O/W) or sediment (W/O). This sedimentation or creaming front can be seen in *BS* signals evolution,[36,37] leading eventually to an increase in transmitted light in the continuous phase region as droplets migrate, i.e. bottom for O/W and top for W/O. Secondly, aggregation and coalescence of droplets also contribute to emulsion destabilization. Droplet aggregation corresponds to droplets sticking together but no increase in diameter. On the other hand, coalescence corresponds to droplets merging together, forming larger droplets until the internal phase is eventually released as a separate phase. Both aggregation and coalescence phenomena cause the apparent number of dispersed objects to decrease as a droplet agglomerate will scatter light the same way as one object would. Additionally, Ostwald ripening, causing smaller droplets to diffuse into larger ones until total dissolution, also contribute to decreasing the droplet number. Consequently, *BS* light signal, directly dependent on the number of dispersed objects, decreases. Examples in the case of cyclohexane W/O and dodecane O/W emulsions at WOR 50-50 are given in Figure 5. In both those emulsions, no internal phase release is visible. This would correspond to *T* signal increasing at the bottom (W/O) or at the top (O/W) of the sample. Additionally, the stability profile for the octane/water emulsion is represented in Figure 5 (middle). At first, this system forms an O/W emulsion, but quickly evolving towards a W III microemulsion. This evolution is visible as both water and oil phases become clear with an increase in *T* signal while the microemulsion phase remains turbid.

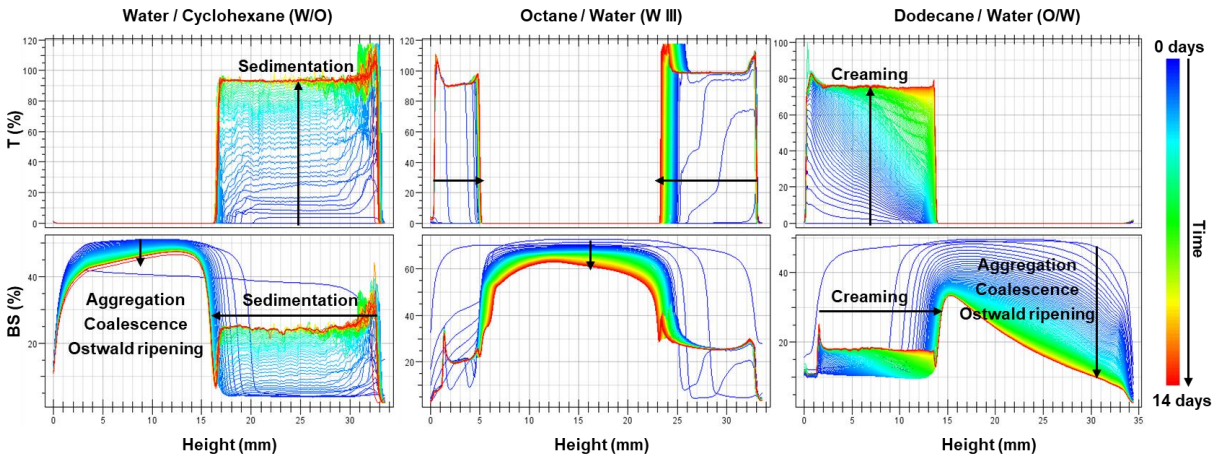

Figure 5. *T* and *BS* light signals over time for water / cyclohexane (left), octane / water (middle) and dodecane / water (right) emulsions (WOR = 50-50, 1% $C_{12}Gly_2$). Creaming and sedimentation fronts are represented by horizontal arrows on *BS* signals and vertical arrows on *T* evolution. Coalescence and/or aggregation and/or Ostwald ripening are visible as *BS* decreases over time.

For every WOR investigated in this work, the most unstable emulsions are the ones formed with octane: fast increase in *T* signal at the top of the sample is observed in O/W emulsions for EACN = 8 (octane) evolving towards a W III microemulsion system for WOR 30-70, 50-50 and 70-30. The evolution of internal phase separation over time is presented in Figure S3 of the Supplementary Information. At low water content (WOR 20-80), excess oil is quickly released due to facilitated droplet coalescence. Inversely, at high water content (WOR 80-20), oil droplets cream but the oil content being low, phase separation is only slightly visible with non-zero *T* light in the upper part of the sample. Also, emulsions prepared with hexane (HLD_N = 2.2) and decane (HLD_N = -1.8), i.e. with EACN close to PACN, show important internal phase separation.

The volume percentage of released internal phase after 14 days shown in Figure 6 is in accordance with the expected evolution in the frame of HLD_N theory.[7,33] The PACN of $C_{12}Gly_2$ being of 8.2, the most unstable emulsions are formed with octane (HLD_N = 0.2). This is verified at WOR ranging from 20-80 to 80-20. For WOR 70-30, the volume of released internal phase is comparable for hexane, octane and decane emulsions. However, the kinetics of destabilization shown in Figure 6 confirms that the octane emulsion is much les stable than the hexane and decane ones.

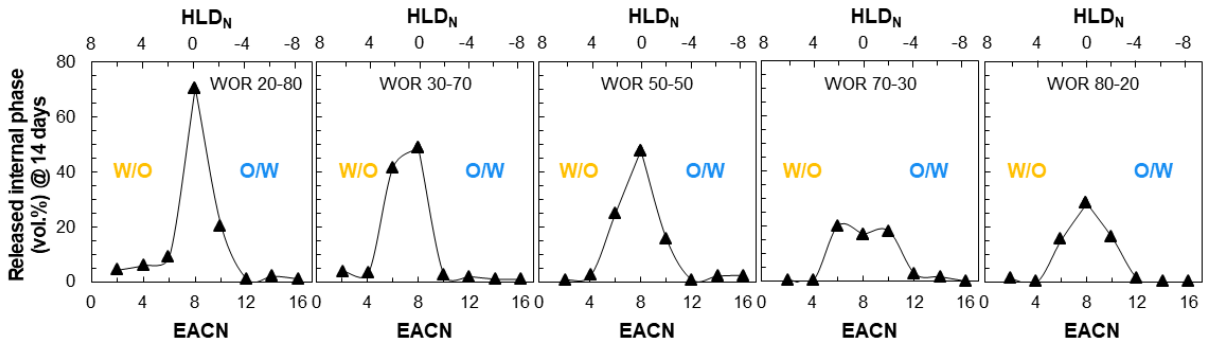

Figure 6. Relative volume of released internal phase after 14 days for emulsions prepared with 1% $C_{12}Gly_2$ and by varying the nature of the oil and the Water-to-Oil Ratio (WOR).

Phenomena of coalescence and/or flocculation and/or Ostwald ripening can be quantified by looking at the *BS* light variations. A decrease in *BS* while *T* remains null indicates a decrease in the number of light scattering objects as expressed in equation (3), caused by combinations of these objects. A way to discriminate both phenomena is to re-measure droplet size after stability monitoring: if droplet size is unchanged, droplets flocculate without coalescing or dissolving into one-another. After gentle re-agitating the emulsions to disperse the droplets homogeneously in the sample, size was re-measured. Results are presented in Figure 7.

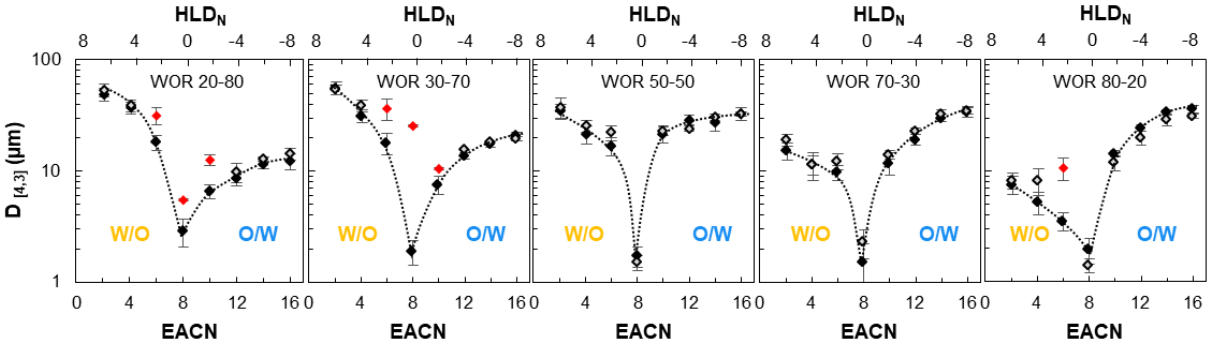

Figure 7. Droplet $D_{[4,3]}$ of emulsions containing 1 wt.% $C_{12}Gly_2$ and prepared by varying the nature of the oil (EACN) and the Water-to-Oil Ratio at initial state (◆) and after 14 days (◇). Significantly different diameters are represented in red (◆).

For most samples, droplet size did not change significantly over 14 days, indicating that droplet coalescence and Ostwald ripening were not prominent destabilizing phenomena. Significantly droplet size changes are observed in hexane W/O emulsions (WOR 20-80, 30-70 and 80-20), decane O/W emulsions (WOR 20-80 and 30-70) and octane O/W emulsions (WOR 20-80 and 30-70). Given the rapid destabilization of octane-based O/W emulsions, it was expected that droplet size would change rapidly for these emulsions. However, surprisingly, it turned out that the droplet size re-measured after 14 days had not changed significantly, whether the WOR was equal to 50-50 or 80-20. A tentative explanation for this unexpected result would be that due to the ultra-low O/W interfacial tension, the gentle stirring would be sufficient to re-form very small droplets and restore the original state of the emulsion.

3.2.2. Influence of process on the droplet size and the stability of emulsions

In this paragraph, emulsions with WOR 50-50 were prepared either by mechanical stirring at room temperature using an Ultra-turrax® or by thermally-induced dynamic phase inversion. In the previous section, the transition from a direct O/W emulsion to a reverse W/O emulsion was obtained by decreasing the EACN value of the oil. More generally, any variable (PACN,

EACN, T, S) involved in equation (1) of the HLD_N can be employed to induce such a phase inversion. However, the temperature is the variable most often used with thermosensitive surfactants because it is reversible and allows significant variations of the HLD_N without requiring a modification of the composition of the SOW system under study. Figure 3a shows the evolution of the PIT as a function of the EACN of a series of n-alkanes. The PITs of the two cycloalkanes could not be measured because they are below zero. Thanks to the correlation line between PIT and EACN, their PITs were estimated by extrapolation from their already known EACNs. The PITs of the various oils and the corresponding EACNs are reported in Table 2.

Table 2. PIT and EACN values of a series of linear and cyclic alkanes.

Oil	EACN	PIT
cyclohexane	2.1	-17.8°C[a]
cyclooctane	4.1	-3.7°C[a]
hexane	6	9.7°C[a]
heptane	7	16.8°C
octane	8	23.9°C
nonane	9	30.9°C
decane	10	38.0°C
dodecane	12	52.1°C
tetradecane	14	66.2°C[a]

[a] Extrapolated values from Figure 3a

The so-called “transitional phase inversion” of SOW systems is accompanied by a progressive evolution of the curvature of the interfacial film and of the HLD_N value. At the optimal temperature, the mean curvature and the HLD_N are exactly equal to zero and the O/W interfacial tension exhibits a deep minimum. At this particular temperature, phases are sheared very efficiently due to minimal interfacial tension of the order of 10^{-2}-10^{-5} $mN.m^{-1}$,[13,38] and the resulting droplets are much smaller than for SOW systems mechanically emulsified at room temperature.[39,40] In the case of octane, the droplet size is comparable with the two emulsification methods because the HLD_N=0 point is obtained at room temperature during mechanical emulsification. Droplet size of PIT emulsified systems are in the same order of magnitude (1-3 µm) and they are higher than for W/O emulsion obtained with hexane. Destabilization is also visible in Figure 8b with the increase of released internal phase after 14 days: a peak in instability is reached for octane emulsion, which separates faster than other emulsions for which stability is comparable with little dephasing (< 5%) observed after 14 days.

The instability of octane emulsion is a consequence of the vicinity of the room temperature and the PIT, making that the system has an HLD_N close to 0. For the others oils, no matter the morphology (W/O or O/W) the final temperature of the system is far enough of the PIT condition and the smaller size of droplets obtained contributes to decreasing creaming and sedimentation processes while Brownian motion contributes to avoiding agglomeration and thus coalescence.[41] These results shows the importance of the emulsification protocol. Emulsions obtained only by mechanical agitation at 25°C with decane and hexane as oils are unstable because their EACN is not far away of the PACN (8.2) and the HLD_N is close to 0 (negative and positive respectively). When the same systems are prepared by the PIT method, the emulsions are more stable even if the formulation condition (HLD_N) remains the same, because the droplet size is smaller. Also, narrow size distributions are obtained using the PIT process, attributed to the efficient shearing during phase inversion, as illustrated in Figure S5 of the Supplementary Information in the case of dodecane emulsions.

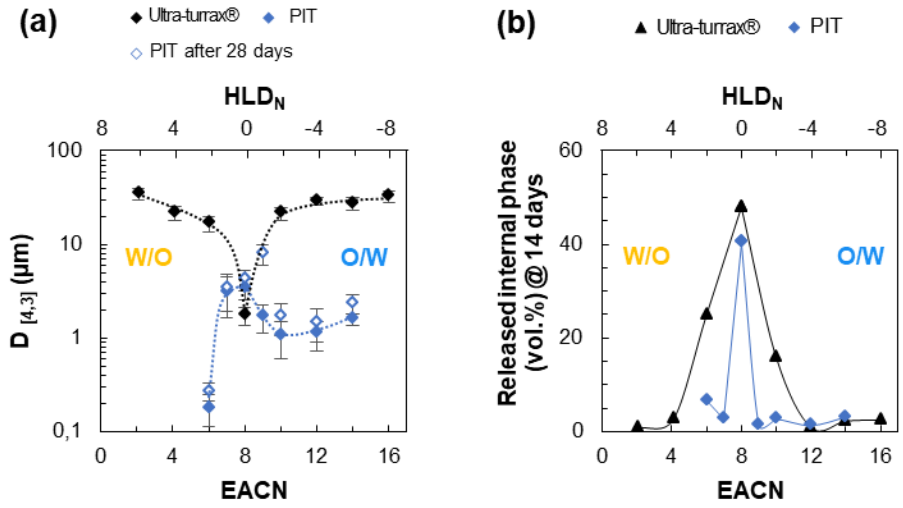

Figure 8. Evolution of (a) droplets $D_{[4,3]}$ and (b) relative volume of released internal phase after 14 days in emulsions with oils of various EACN prepared by varying the emulsification process (WOR 50-50, 1% $C_{12}Gly_2$). All represented oils are detailed in Table 2.

3.2.3. Influence of the surfactant concentration on the droplet size of emulsions based on cosmetic oils

Finally, the influence of another composition variable (the surfactant concentration) and other formulation variable (other oils different to alkanes or cycloalkanes) are studied. It is a matter of fact that increasing the surfactant concentration provides a better covering of droplets surface. Two cosmetic oils, namely octyl octanoate (EACN = 8.1) [42] which is an ester used in skin care products as an emollient and as flavouring agent in food products,[43–45] and squalane (EACN = 24.4) [26] which is a branched alkane used as an emollient in skin care products, were used as oil phases in this series of emulsions.

Figure 9a shows that granulometry evolution with the oil EACN is in accordance with the previously observed tendency at 1% $C_{12}Gly_2$. By increasing $C_{12}Gly_2$ concentration from 1% to 3%, not only droplet size is decreased as shown in see Figure 9a, but stability is also improved. The interface being better stabilized, significant phase separation (> 5 vol.%) was observed after 14 days only in the case of octane and octyl octanoate (HLD_N ~ 0) while other emulsions remain with lower separation percentages. Also, diameter evolution after 14 days shows that no significant coalescence occurs, except for HLD_N ~ 0. As depicted in Figure 9b, the main stability improvement compared to the 1% $C_{12}Gly_2$ emulsion series is observed for hexane and decane emulsions.

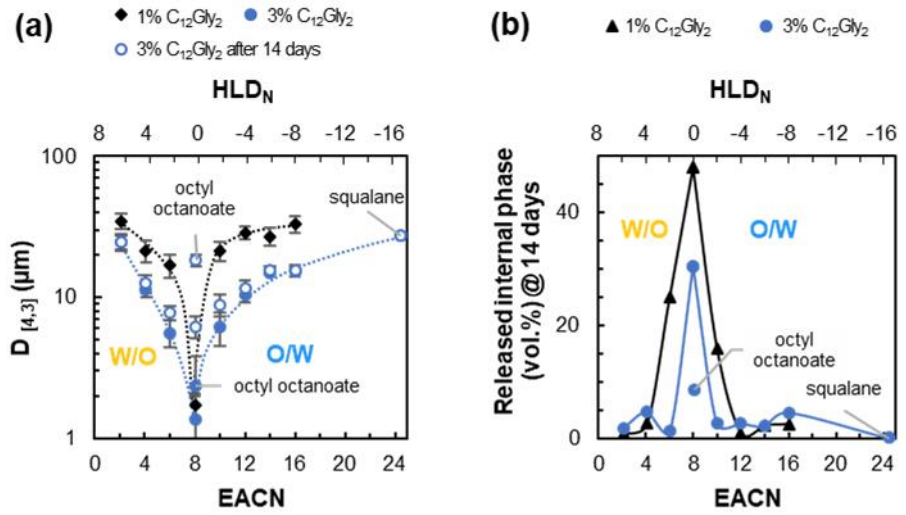

Figure 9. Evolution of (a) droplets $D_{[4,3]}$ and (b) relative volume of released internal phase after 14 days in emulsions with oils of various EACN prepared by varying the $C_{12}Gly_2$ surfactant concentration from 1% to 3% (WOR 50-50, emulsified using the Ultra-turrax® procedure). All represented oils are detailed in Table 2 except octyl octanoate and squalane that are clearly indicated.

Octyl octanoate (HLD_N = 0.1) initial droplet size concurs with that of octane (HLD_N = 0.2) droplets. However, the octyl octanoate emulsion destabilizes slower: droplet size increases significantly but internal phase release appears only after 11 days and remains inferior after 14 days, see Figure 9b. For that particular oil, the droplet size evolution after 14 days is important. This may be attributed to the higher solubility of octyl octanoate in water compared to alkanes, due to its polarity. Solubility of the dispersed phase into the continuous one favours Ostwald ripening as destabilization phenomenon. It also decreases the surfactant availability at the interface and thus decreases the droplet covering, increasing droplet granulometry. Also, the density of octyl octanoate is higher than that of octane (0.870 vs. 0.703, respectively), slowing down the creaming process. The HLD_N value of the squalane emulsion being of -16.2, the formed O/W droplets are relatively large in accordance with the general tendency observed with other alkanes and cycloalkanes, and the emulsion is the most stable against coalescence. No significant droplet size evolution or internal phase release are observed.

3.3. Nanoemulsification of oils by frolicking inside the Formulation-Composition map

In this paragraph we will illustrate, on a practical example, how the Formulation-Composition map can be exploited to design emulsions with the desired morphology and particle size while minimizing thermal and mechanical energy. According to Figure 4, a dodecane/water emulsion containing 70 vol.% of water would form droplets of about 25 µm if prepared by mechanical agitation. The PIT process was shown to form smaller droplets but requires energy to heat the mixture above the PIT value. This energy can be minimized by heating the minimum amount of water/dodecane/$C_{12}Gly_2$, then adding the required amount of water to reach the 70 vol.% content and quickly cooling down the system to quench droplet evolution. The principle of this strategy is shown in Figure 10a and the monitoring of the conductivity during the thermally induced phase inversion is shown in Figure 10b.

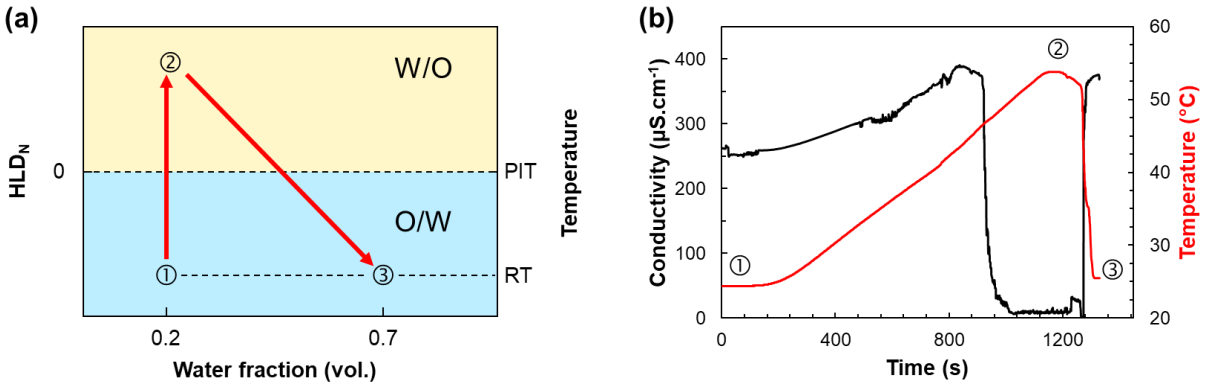

Figure 10. Nanoemulsification of the $C_{12}Gly_2$/n-Dodecane/Water system (a) Illustration of HLD_N and temperature variations when heating an emulsion (water fraction = 0.2) above PIT and diluting to water fraction = 0.7 with cold water and (b) corresponding conductivity and temperature inversion profiles.

Figure 10b shows the conductivity and temperature profiles. The first inversion (1→2) occurs at 930 s when the PIT of the system is reached and the conductivity decreases. The phase inversion occurs around 47°C, which is slightly lower than for the same system with WOR 50-50 (PIT = 52.1°C) as expected.[46] The second inversion (2→3) is obtained when the cool water was added into the system to form again a O/W emulsion, increasing the conductivity. The obtained size of the emulsion ($D_{[4,3]}$ = 1.4 µm) is significantly lower than with a simple agitation ($D_{[4,3]}$ = 8.6 µm).

Similar experiment carried out with 3% $C_{12}Gly_2$ yielded even smaller droplets, in accordance with a better covering of O/W interface. Assuming that most of the surfactant is only localized at the interface (negligible solubilization in water and oil phases), the theoretical droplet diameter would be of 264 nm with 1% $C_{12}Gly_2$ and of 88 nm with 3% $C_{12}Gly_2$. This calculation considers all droplets being of the same size and details about calculations are given in

Supplementary Information. Experimental results show that droplets are larger than expected for 1% $C_{12}Gly_2$ ($D_{[4,3]}$ = 1.44 µm) but match well the calculations for 3% $C_{12}Gly_2$ ($D_{[4,3]}$ = 114 nm). Indeed, the order of magnitude is identical and the $D_{[4,3]}$ statistical value favours the ponderation of larger droplets whereas theoretical calculations consider monodisperse populations. The difference observed for 1% $C_{12}Gly_2$ could be due to the lesser availability of $C_{12}Gly_2$ to quickly stabilize the newly created interface when the cold water is added, whereas this process is faster when using 3% $C_{12}Gly_2$. Using the same approach, any oil, for which the PIT value is within the accessible temperature range, could be emulsified in order to get nanoemulsions adjusting the surfactant concentration.

4. Conclusion

Emulsions characteristics depend on 3 types of variables: formulation variables (Surfactant, Oil, Temperature and Salinity), composition variables (WOR and wt.% of surfactant) and process variables (Stirring and protocol used). Formulation variables are accounted for in the HLD_N equation (1). The emulsifying properties of the bio-based 1-*O*-dodecyl diglyceryl ether surfactant were investigated by using the HLD_N framework. All the coefficients of the HLDN equation were determined for $C_{12}Gly_2$ and the results showed that $C_{12}Gly_2$ is about 3 times less sensitive to variations in temperature and salinity than the polyethoxylated alcohols C_iE_j (τ = 0.14°C^{-1} against 0.40°C^{-1} and δ = 0.53 wt.%$^{-1}$ against 0.16% wt.%$^{-1}$ for $C_{12}Gly_2$ and $C_{10}E_4$ respectively). A PACN value of 8.2 for $C_{12}Gly_2$ was determined by dynamic PIT evolution with ACN, in accordance with literature values using the PIT-slope method.[28] The lower sensitivity to temperature and salinity of C12Gly2 compared to C10E4 is explained by the presence of 2 hydroxyl groups instead of just one. Indeed, the OH groups establish much stronger hydrogen bonds with water than the ether functions which are easier to break thermally.

A general tendency in the evolution of emulsion granulometry and stability was demonstrated with alkanes and cycloalkanes and verified with two more complex oils, namely octyl octanoate (EACN = 8.1, HLD_N = 0.1) and squalane (EACN = 24.4, HLD_N = -16.2). Emulsions prepared by varying the nature of the oil (EACN) showed significant differences in granulometry and stability. The minimum of interfacial tension between oil and water being attained for EACN = PACN, the formation of smaller droplets (about 1 µm) is favoured when using octane (ACN = 8) or octyl octanoate (EACN = 8.1). Whatever the value of the WOR, the droplet size increases as oil EACN differs from the surfactant PACN. For HLD_N = 0, the affinity of $C_{12}Gly_2$ is equivalent for both water and oil at 25°C, and the interface curvature is close to 0, causing droplets to destabilize quickly. Also, the kinetics of internal phase release is faster with octane than any other investigated oil, regardless of the emulsion WOR. The

evolution of stability with EACN is in accordance with HLD_N as stability increases as HLD_N differs from 0 and EACN differs from 8.2.

Increasing the surfactant concentration from 1% to 3% had little impact on octane emulsion granulometry but reduced by more than 10 µm the droplet size for other emulsions due to better droplet interface covering. Stability was also improved with less than 5 vol.% of released internal phase after 14 days, except for $HLD_N \sim 0$ emulsions. The same way, emulsions prepared by PIT allowed forming droplets inferior to 2 µm for $HLD_N \neq 0$, much more stable over time than emulsions prepared by Ultra-turrax® as droplet flocculation and coalescence are limited by Brownian motion. This work and previous results about foaming properties and microemulsions[28] allows present the $C_{12}Gly_2$ as very promising nonionic surfactant. It is a good emulsifier and foaming agent with the advantage compared to $C_{12}E_5$-$C_{12}E_6$ to be a better foaming agent. In comparison with alkyl polyglucosides (APG), which are good foaming agents and emulsifiers, the $C_{12}Gly_2$ allows getting phase inversion using temperature as formulation variable while APG do not (insensitive to temperature changes). The influence of the alkyl chain and the number of glycerol groups of C_iGly_n on the emulsifying and foaming properties must be further studied in order to clearly define the role of these promising molecules in the substitution of polyethoxylated surfactants.

Acknowledgements

Chevreul Institute (FR 2638), Ministère de l'Enseignement Supérieur et de la Recherche, Région Hauts-de-France, and FEDER are acknowledged for supporting and funding partially this work. We are deeply grateful to Prof. Marc Lemaire and Dr. Raphael Lebeuf for the donation of samples of the $C_{12}Gly_2$ surfactant.

References

[1] H. Sagitani, Y. Hayashi, M. Ochiai, Solution properties of homogeneous polyglycerol dodecyl ether nonionic surfactants, JAOCS. 66 (1989) 146–152. https://doi.org/10.1007/BF02661806.
[2] K. Shinoda, M. Fukuda, A. Carlsson, Characteristic solution properties of mono-, di-, and triglyceryl alkyl ethers: lipophobicity of hydrophilic groups, Langmuir. 6 (1990) 334–337. https://doi.org/10.1021/la00092a007.
[3] W. Ostwald, Beiträge zur Kenntnis der Emulsionen, Kolloid Z. 6 (1910) 103–109.
[4] W.D. Bancroft, The Theory of Emulsification, V, J. Phys. Chem. 17 (1913) 501–519. https://doi.org/10.1021/j150141a002.
[5] W.D. Bancroft, The Theory of Emulsification, VI, J. Phys. Chem. 19 (1915) 275–309. https://doi.org/10.1021/j150157a002.
[6] J.-L. Salager, Guidelines for the Formulation, Composition and Stirring to Attain Desired Emulsion Properties (Type, Droplet Size, Viscosity and Stability), in: Surfactants in Solution, CRC Press, New York, 1996: pp. 261–295.
[7] J.-L. Salager, R. Antón, J. Bullón, A. Forgiarini, R. Marquez, How to use the normalized hydrophilic-lipophilic deviation (HLD_N) concept for the formulation of equilibrated and emulsified surfactant-oil-water systems for cosmetics and pharmaceutical products, Cosmetics. 7 (2020) 57. https://doi.org/10.3390/cosmetics7030057.
[8] J.-M. Aubry, J.F. Ontiveros, J.-L. Salager, V. Nardello-Rataj, Use of the normalized hydrophilic-lipophilic-deviation (HLD_N) equation for determining the equivalent alkane carbon number (EACN) of oils and the preferred alkane carbon number (PACN) of nonionic surfactants by the fish-tail method (FTM), Adv. Colloid Interface Sci. 276 (2020) 102099. https://doi.org/10.1016/j.cis.2019.102099.
[9] J.L. Salager, J.C. Morgan, R.S. Schechter, W.H. Wade, E. Vasquez, Optimum Formulation of Surfactant/Water/Oil Systems for Minimum Interfacial Tension or Phase Behavior, SPE J. 19 (1979) 107–115. https://doi.org/10.2118/7054-PA.
[10] W. Kunz, F. Testard, T. Zemb, Correspondence between Curvature, Packing Parameter, and Hydrophilic−Lipophilic Deviation Scales around the Phase-Inversion Temperature, Langmuir. 25 (2009) 112–115. https://doi.org/10.1021/la8028879.
[11] M.E. Hayes, M. Bourrel, M.M. El-Emary, R.S. Schechter, W.H. Wade, Interfacial Tension and Behavior of Nonionic Surfactants, SPE J. 19 (1979) 349–356. https://doi.org/10.2118/7581-PA.
[12] J.L. Salager, M. Bourrel, R.S. Schechter, W.H. Wade, Mixing Rules for Optimum Phase-Behavior Formulations of Surfactant/Oil/Water Systems, SPE J. 19 (1979) 271–278. https://doi.org/10.2118/7584-PA.
[13] T. Sottmann, R. Strey, Ultralow interfacial tensions in water–n-alkane–surfactant systems, J. Chem. Phys. 106 (1997) 8606–8615. https://doi.org/10.1063/1.473916.
[14] C. Pierlot, J.F. Ontiveros, M. Catté, J.-L. Salager, J.-M. Aubry, Cone–Plate Rheometer as Reactor and Viscosity Probe for the Detection of Transitional Phase Inversion of Brij30–Isopropyl Myristate–Water Model Emulsion, Ind. Eng. Chem. Res. 55 (2016) 3990–3999. https://doi.org/10.1021/acs.iecr.6b00399.
[15] J.L. Salager, M. Miñana-Pérez, J.M. Andérez, J.L. Grosso, C.I. Rojas, I. Layrisse, Surfactant-Oil-Water Systems Near the Affinity Inversion Part II: Viscosity of Emulsified

Systems, J. Dispers. Sci. Technol. 4 (1983) 161–173. https://doi.org/10.1080/01932698308943361.
[16] K. Shinoda, H. Arai, The Correlation between Phase Inversion Temperature In Emulsion and Cloud Point in Solution of Nonionic Emulsifier, J. Phys. Chem. 68 (1964) 3485–3490. https://doi.org/10.1021/j100794a007.
[17] T. Gibson, Phase-Transfer Synthesis of Monoalkyl Ethers of Oligoethylene Glycols, J. Org. Chem. 45 (1980) 1095–1098. https://doi.org/10.1021/jo01294a034.
[18] J.C. Lang, R.D. Morgan, Nonionic surfactant mixtures. I. Phase equilibria in $C_{10}E_4$–H_2O and closed-loop coexistence, J. Chem. Phys. 73 (1980) 5849–5861. https://doi.org/10.1063/1.440028.
[19] J. Schlarmann, C. Stubenrauch, R. Strey, Correlation between film properties and the purity of surfactants, Phys. Chem. Chem. Phys. 5 (2003) 184–191. https://doi.org/10.1039/B208899C.
[20] L. Delforce, New methodologies for characterizing particles, complex oils and surfactants : relations between chemical structure, physicochemical properties and applicative properties, PhD thesis, Université de Lille, 2022. https://theses.hal.science/tel-03998778.
[21] G. Lemahieu, J.F. Ontiveros, N. Terra Telles Souza, V. Molinier, J.-M. Aubry, Fast and accurate selection of surfactants for enhanced oil recovery by dynamic Salinity-Phase-Inversion (SPI), Fuel. 289 (2021) 119928. https://doi.org/10.1016/j.fuel.2020.119928.
[22] G. Lemahieu, J.F. Ontiveros, T. Gaudin, V. Molinier, J.-M. Aubry, The Salinity-Phase-Inversion method (SPI-slope): A straightforward experimental approach to assess the hydrophilic-lipophilic-ratio and the salt-sensitivity of surfactants, J. Colloid Interface Sci. 608 (2022) 549–563. https://doi.org/10.1016/j.jcis.2021.09.155.
[23] O. Mengual, G. Meunier, I. Cayré, K. Puech, P. Snabre, TURBISCAN MA 2000: multiple light scattering measurement for concentrated emulsion and suspension instability analysis, Talanta. 50 (1999) 445–456. https://doi.org/10.1016/S0039-9140(99)00129-0.
[24] Y. Shi, W. Dayoub, A. Favre-Réguillon, G.-R. Chen, M. Lemaire, Straightforward selective synthesis of linear 1-O-alkyl glycerol and di-glycerol monoethers, Tetrahedron Lett. 50 (2009) 6891–6893. https://doi.org/10.1016/j.tetlet.2009.09.134.
[25] W.H. Wade, J.C. Morgan, R.S. Schechter, J.K. Jacobson, J.L. Salager, Interfacial Tension and Phase Behavior of Surfactant Systems, Soc. Pet. Eng. J. 18 (1978) 242–252. https://doi.org/10.2118/6844-PA.
[26] S. Queste, J.L. Salager, R. Strey, J.M. Aubry, The EACN scale for oil classification revisited thanks to fish diagrams, J. Colloid Interface Sci. 312 (2007) 98–107. https://doi.org/10.1016/j.jcis.2006.07.004.
[27] S. Burauer, T. Sachert, T. Sottmann, R. Strey, On microemulsion phase behavior and the monomeric solubility of surfactant, Phys. Chem. Chem. Phys. 1 (1999) 4299–4306. https://doi.org/10.1039/A903542G.
[28] J.F. Ontiveros, C. Pierlot, M. Catté, J.-L. Salager, J.-M. Aubry, Determining the Preferred Alkane Carbon Number (PACN) of nonionic surfactants using the PIT-slope method, Colloids Surf. A Physicochem. Eng. Asp. 536 (2018) 30–37. https://doi.org/10.1016/j.colsurfa.2017.08.002.
[29] J.D. Roberts, M.C. Caserio, Alcohols and ethers, in: Basic Principles of Organic Chemistry, Second Edition, W. A. Benjamin, Inc., Menlo Park, CA, 1977. https://doi.org/10/BPOCchapter9.pdf.
[30] J. Chirife, S.L. Resnik, Unsaturated Solutions of Sodium Chloride as Reference Sources of Water Activity at Various Temperatures, J. Food Sci. 49 (1984) 1486–1488. https://doi.org/10.1111/j.1365-2621.1984.tb12827.x.
[31] J.-L. Salager, R. Anton, J.-M. Aubry, Formulation des émulsions par la méthode du HLD, Tech. L'Ingénieur. (2006). https://doi.org/10.51257/a-v1-j2158.
[32] M. Bourrel, J.L. Salager, R.S. Schechter, W.H. Wade, A correlation for phase behavior of nonionic surfactants, J. Colloid Interface Sci. 75 (1980) 451–461. https://doi.org/10.1016/0021-9797(80)90470-1.

[33] J.-L. Salager, The fundamental basis for the action of a chemical dehydrant. Influence of the physical and chemical formulation on the stability of an emulsion, Int. Chem. Eng. 30 (1990) 103–116.
[34] J.-L. Salager, M. Perez-Sanchez, Y. Garcia, Physicochemical parameters influencing the emulsion drop size, Colloid Polym Sci. 274 (1996) 81–84. https://doi.org/10.1007/BF00658913.
[35] L.-I. Tolosa, A. Forgiarini, P. Moreno, J.-L. Salager, Combined Effects of Formulation and Stirring on Emulsion Drop Size in the Vicinity of Three-Phase Behavior of Surfactant−Oil Water Systems, Ind. Eng. Chem. Res. 45 (2006) 3810–3814. https://doi.org/10.1021/ie060102j.
[36] L. Zheng, C. Cao, R.-Y. Li, L.-D. Cao, Z.-L. Zhou, M. Li, Q.-L. Huang, Preparation and characterization of water-in-oil emulsions of isoprothiolane, Colloids Surf. A Physicochem. Eng. Asp. 537 (2018) 399–410. https://doi.org/10.1016/j.colsurfa.2017.10.031.
[37] K. Peng, X. Wang, L. Lu, J. Liu, X. Guan, X. Huang, Insights into the Evolution of an Emulsion with Demulsifying Bacteria Based on Turbiscan, Ind. Eng. Chem. Res. 55 (2016) 7021–7029. https://doi.org/10.1021/acs.iecr.6b01347.
[38] H. Kunieda, S.E. Friberg, Critical Phenomena in a Surfactant/Water/Oil System. Basic Study on the Correlation between Solubilization, Microemulsion, and Ultralow Interfacial Tensions, BCSJ. 54 (1981) 1010–1014. https://doi.org/10.1246/bcsj.54.1010.
[39] T. Engels, T. Förster, W. von Rybinski, The influence of coemulsifier type on the stability of oil-in-water emulsions, Colloids Surf. A Physicochem. Eng. Asp. 99 (1995) 141–149. https://doi.org/10.1016/0927-7757(95)03132-W.
[40] S. Friberg, C. Solans, Emulsification and the HLB-temperature, J. Colloid Interface Sci. 66 (1978) 367–368. https://doi.org/10.1016/0021-9797(78)90319-3.
[41] T. Tadros, P. Izquierdo, J. Esquena, C. Solans, Formation and stability of nano-emulsions, Adv. Colloid Interface Sci. 108–109 (2004) 303–318. https://doi.org/10.1016/j.cis.2003.10.023.
[42] J.F. Ontiveros, C. Pierlot, M. Catté, V. Molinier, A. Pizzino, J.-L. Salager, J.-M. Aubry, Classification of ester oils according to their Equivalent Alkane Carbon Number (EACN) and asymmetry of fish diagrams of $C_{10}E_4$/ester oil/water systems, J. Colloid Interface Sci. 403 (2013) 67–76. https://doi.org/10.1016/j.jcis.2013.03.071.
[43] Joint FAO/WHO Expert Committee on Food Additives (JECFA) - Octyl octanoate, Food and Agriculture Organization of the United Nations. (n.d.). https://www.fao.org/food/food-safety-quality/scientific-advice/jecfa/jecfa-flav/details/en/c/25/ (accessed July 27, 2022).
[44] Commission Implementing Regulation (EU) No 872/2012 of 1 October 2012 adopting the list of flavouring substances provided for by Regulation (EC) No 2232/96 of the European Parliament and of the Council, introducing it in Annex I to Regulation (EC) No 1334/2008 of the European Parliament and of the Council and repealing Commission Regulation (EC) No 1565/2000 and Commission Decision 1999/217/EC Text with EEA relevance, 2012. http://data.europa.eu/eli/reg_impl/2012/872/oj/eng (accessed July 27, 2022).
[45] G. Zocchi, Skin-Feel Agents, in: Handbook of Cosmetic Science and Technology, 1st Edition, CRC Press, Boca Raton, 2001.
[46] A. Pizzino, V. Molinier, M. Catté, J.F. Ontiveros, J.-L. Salager, J.-M. Aubry, Relationship between phase behavior and emulsion inversion for a well-defined surfactant ($C_{10}E_4$)/n-octane/water ternary system at different temperatures and water/oil ratios, Ind. Eng. Chem. Res. 52 (2013) 4527–4538. https://doi.org/10.1021/ie302772u.